

**NEW INSIGHTS INTO THE STEREOCHEMICAL REQUIREMENTS OF THE
BRADYKININ B1 RECEPTOR ANTAGONISTS BINDING**

Cecylia S. Lupala, Patricia Gomez-Gutierrez and Juan J. Perez

Dept. of Chemical Engineering

Universitat Politecnica de Catalunya

ETSEIB. Av. Diagonal, 647; 08028 Barcelona, Spain

Abstract

Bradykinin (BK) is a nonapeptide involved in several pathophysiological conditions including among others, septic and haemorrhagic shock, anaphylaxis, arthritis, rhinitis, asthma, inflammatory bowel disease. Accordingly, BK antagonists have long been sought after for therapeutic intervention. Action of BK is mediated through two different G-protein coupled receptors known as B1 and B2. Although there are several B1 antagonists reported in literature, their pharmacological profile is not yet optimal so that new molecules need to be discovered. In the present work we have constructed an atomistic model of the B1 receptor and docked diverse available non-peptide antagonists in order to get a deeper insight into the structure-activity relationships involving binding to this receptor. The model was constructed by homology modelling using the chemokine CXC4 and bovine rhodopsin receptors as template. The model was further refined using molecular dynamics for 600 ns with the protein embedded in a POPC bilayer. From the refinement process we obtained an average structure that was used for docking studies using the Glide software. Antagonists selected for the docking studies include Compound 11, Compound 12, Chroman28, SSR240612, NPV-SAA164 and PS020990. The results of the docking study underline the role of specific receptor residues in ligand binding. The results of this study permitted to define a pharmacophore that describes the stereochemical requirements of antagonist binding, and can be used for the discovery of new compounds.

Introduction

Bradykinin (BK) is a nonapeptide with sequence Arg¹-Pro²-Pro³-Gly⁴-Phe⁵-Ser⁶-Pro⁷-Phe⁸-Arg⁹, involved in several pathophysiological conditions including among others, septic and hemorrhagic shock, anaphylaxis, arthritis, rhinitis, asthma, inflammatory bowel disease. Accordingly, BK antagonists have long been sought after for therapeutic intervention. Action of BK is mediated through two different G-protein coupled receptors known as B1 and B2. The former is up-regulated during inflammation episodes or tissue trauma whereas the latter, is constitutively expressed in a variety of cell types, mediating most physiological actions of bradykinin [1-3]. Most attempts in the past were devoted to develop antagonists of the B2 receptor [4], with a stride made after the market release of the peptide antagonist Icatibant [5,6]. More recently, the demonstrated implication of B1 in establishing and maintaining the signaling of chronic and inflammatory pain [3,7,8], as well as in hyperalgesia and leucocyte infiltration through the activation of a cytokine network, has increased the interest in finding small molecule B1 antagonists for the treatment of both pain and inflammation [9-13]. Despite of these efforts there is no drug currently in the market designed to antagonize the B1 bradykinin receptor.

The goal of the present work is to carry out a structure-activity study of B1 antagonism, taking into account the stereochemical features of diverse non-peptide antagonists described in the literature and understand how these features translate into ligand anchoring points and complementary regions of the receptor, through the analysis of the respective ligand-receptor complexes. For this purpose we selected a set of compounds from the literature covering the maximal structural diversity as shown in Figure 1. The six compounds selected for the present study include Merck compounds 11 (1) [14-16] and 12 (2) [17]; Novartis NPV-SAA164 (3) [18,19]; Amgen Chroman28 (4) [20,21]; Sanofi-Synthelabo SSR240612 (5) [22] and Pharmacopeia PS020990 (6) [23]. The selected compounds were docked onto a refined model of the BK B1 receptor constructed by homology modeling, following the procedure explained in the methods section, being the complexes further analyzed for their ligand-receptor interactions. The outcome of this study is summarized on a 3D pharmacophore that explains the observed structure-activity results and provides insights into the discovery of novel molecules with antagonistic profile at the B1 bradykinin receptor.

Methodology

Computational methods

A starting model of the human BK B1 receptor was constructed by homology modeling using the chemokine CXCR4 receptor as template (pdb entry code 3ODU) [24]. This template was selected among those GPCRs whose crystallographic structure is available based on its proximity to B1 receptor in the GPCRs phylogenetic tree. The sequences of the two receptors were aligned, taking into account the conserved motifs found in all GPCRs, as well as the location of the disulfide bridges. These motifs, together with salt bridges are important factors in constraining the conformation of the extracellular and transmembrane domains of the receptor. Sequences were found to share about 25% sequence identity. Additionally, since the chemokine CXCR4 lacks the expected helical TM8, residues of the B1 receptor known to be in the TM8, starting from the highly conserved NPXXY motif [25] were modeled using the corresponding segment of the crystal structure of bovine rhodopsin (pdb entry code 1GZM) [26]. From the aligned sequences and the template backbone, a starting model of the receptor was constructed using the Modeller 9 version 8 (9v8) software [27]. Model was validated using the Molecular Operating Environment (MOE) program [28] after checking diverse steric parameters such as side chain rotamers, inter-residue contacts or backbone conformations.

In a subsequent step, compound 11 (1 in Figure 1) was docked into the starting model for receptor refinement using the GLIDE software [29]. The choice of this ligand was due to the abundant information available on receptor residues involved in its binding from site directed mutagenesis experiments [14-15]. Finally, the ligand-receptor complex was refined using molecular dynamics of the ligand-receptor complex embedded in a lipid bilayer. Specifically, the protein was embedded in a box consisting in 1-palmitoyl-2-oleoyl-sn-glycero-3-phosphocholine (POPC) lipids and water molecules generated and equilibrated according to the procedure described previously [30]. The box had an initial size of 10.3 x 8.0 x 10.2 nm³ (XYZ), organized in such a way that the bilayer plane was oriented on the XY plane. Before protein insertion, the box contained 256 lipids (corresponding to an area per lipid of 0.64 nm²) and circa 17,000 water molecules. The protein was placed in the center of the box, and the overlapping molecules were removed. Specifically, all water molecules with oxygen atoms closer than 0.40 nm to a non-hydrogen atom of the protein and similarly, all lipid molecules with at least one atom closer than 0.25 nm to a non-hydrogen atom of the protein were removed. This resulted in a final system containing 197 lipids and circa 16,000 water molecules. Removal of these atoms introduced small voids between the protein and water or lipid molecules that disappeared during the first part of the MD simulation, in

which a progressive adjustment of the lipid bilayer and water molecules to the protein takes place. Next, 114 randomly selected water molecules were replaced by 58 sodium and 56 chloride ions, providing a neutral system with a concentration approximately 0.2 M on sodium chloride. This concentration is fairly similar to that found in biological organisms, although they exhibit different intra- and extra-cellular ion concentrations. Sampling was carried out at 300K for 600ns using GROMACS 4.6 package [31]. The final model of the B1 receptor was generated from the average structure of the molecular dynamics trajectory using the last 100 ns. The average structure of the receptor was subsequently minimized in a two-step process using the steepest descent method with a dielectric constant of 2. First, side chains are optimized with the backbone atoms constrained to be subsequently released in a second minimization. This structure was used for further docking studies using the GLIDE [29] software. Due to the flexibility of the ligands, the docking process was carried out using a set of unique conformations resulted from thorough conformational searches. Poses were rank ordered using the XP score function of GLIDE [32]. Final poses of the compounds were decided based on their ranking and fulfillment of site directed mutagenesis information available. Final poses were energy minimized using the steepest decent method with a dielectric constant of 2, using the OPLS-AA force field [31] to get a full relaxation of the ligand-receptor complexes.

Binding assays

B1 antagonism assays were carried out following a protocol described elsewhere [33]. Specifically, compounds were tested on human recombinant bradykinin B1 receptors expressed in CHO cells. Saturation isotherms were obtained with [³H] des-Arg¹⁰-BK (0.35 nM) incubated for 60 minutes at room temperature. Non-specific binding was evaluated by adding desArg⁹[Leu⁸]-BK at 10 μM. Antagonism of unlabeled compounds was measured as a percent inhibition of control specific binding of [³H]-bradykinin obtained in the presence of the test compounds at one concentration using NPC-567 as reference compound.

Results and discussion

Construction and refinement of the 3D model of the B1 receptor

In the absence of a crystallographic structure of the B1 receptor, we proceeded to construct an atomistic model using homology modelling. Although the number of crystallographic structures of GPCRs available has

increased steadily during the last few years, there are still challenges that hinder the availability of new ones, including their low-expression yields, low receptor stability after detergent extraction from native membranes, and high conformational heterogeneity. Under these circumstances homology modelling remains one of the important techniques aimed at constructing 3D models of proteins, however in order for the models constructed to be as accurate as possible the procedure requires a careful choice of the template and a robust refinement procedure [34-36]. This consideration is important since the analysis of the diverse crystallographic structures reveals that although they all share a common seven helix bundle, each structure exhibits specific features that might be relevant for ligand design [37].

Figure 2 shows the alignment of the sequences of the CXCR4 and B1 receptors carried out taking into account the conserved motifs found among GPCRs, as explained in the methods section. This procedure is crucial for the assignment of the transmembrane regions. The N-terminus of the B1 receptor as well as transmembrane regions TM1-TM6 and part in TM7 were constructed using CXCR4 chemokine receptor as a template (pdb entry code 3ODU) [24], while the part in TM7 starting from the conserved motif NPXXY was constructed using bovine rhodopsin as a template (pdb entry code 1GZM) [26]. This information was used as input of the Modeller software that produced a set of models that were subsequently rank ordered based on a scoring function. The final model selected for the refinement process was the one with the least steric conflicts from those that incorporated all the specified constraints considered to be conserved among GPCRs.

As mentioned before, structure refinement was carried out through a molecular dynamics simulation of the receptor embedded in a lipid bilayer. Previous experience on GPCR homology modeling, suggests that the presence of the ligand permits a faster equilibration of the system (data not shown). In this case compound 11 (compound 1 in Figure 1) was docked into the orthosteric site in the starting model. The orthosteric site of the B1 receptor is shown in the context of the B1 receptor in Figure 3. It can be described as a large highly hydrophobic pocket formed by TM2, ECL1 and TM7 including residues Trp-93^{2.60}, Ile-97^{2.64}, Phe-101^{ECL1}, Phe-299^{7.40}, Phe-302^{7.43} on one side of the binding pocket. Interestingly, interactions at this side of the pocket involving Trp-93^{2.60}, Phe-101^{ECL1} and Phe-299^{7.40} are quadrupole-quadrupole interactions. (The Ballesteros-Weinstein notation is used for clarity [38].) On the other side of the binding pocket both polar and hydrophobic residues such as, Asn-114^{3.27}, Arg-202^{5.38} and Tyr-266^{6.51} can be identified. Finally, at the top and mouth of the binding site there are

several polar residues including Glu-196^{5.32}, His-199^{5.35}, Glu-273^{6.58}, Gln-277^{6.62}, Glu-287^{7.28}, Asp-288^{7.29}, Asp-291^{7.32}.

Several docking attempts were carried out using diverse conformations that had been generated automatically as explained in the methods section. The final complex considered for refinement was selected based on the degree of fulfilment of the available site directed mutagenesis studies published in the literature. In a subsequent step, the B1 receptor–compound 11 complex was embedded into a box of a pre-equilibrated bilayer of 1-palmitoyl-2-oleoyl-sn-glycero-3-phosphocholine (POPC) and water and subject to molecular dynamics simulations. The time evolution of the root mean square deviation (rmsd) of the alpha carbons of the whole protein as well as those of the helical bundle subset (data not shown) indicates that equilibration is reached after 300 ns when all the alpha carbons of the protein are considered, whereas equilibration is reached about 50 ns earlier when the helical bundle subset is used in the calculation.

The refined model of the BK B1 receptor was produced from the average structure of the last 100 ns of the molecular dynamics trajectory. Since the receptor structure is expected to exhibit small structural variations around the starting point during the refinement process, we consider that an average structure picks up information of the diverse structures sampled. Moreover, crystallographic structures are average structures in nature. The average structure was subsequently minimized in a two-step process using the steepest descent method with a dielectric constant of 2. First, side chains are optimized with the backbone atoms constrained to be subsequently released in a second minimization. This process was aimed to relax the structure to the nearest minimum in a practical manner, avoiding the minimizer spend most of the minimization process reorienting solvent molecules.

This structure was used for the docking study of the different ligands selected in the present study. Below, we describe the proposed bound conformation of each of the diverse antagonists from the corresponding docking studies on the refined model.

Docking studies of the diverse antagonists selected

Compound 11

Compound 11 (1 in Figure 1) was discovered at Merck in the optimization process of a dihydroquinoxalinone lead previously identified as BK B1 receptor antagonist in an in-house screening process [14]. Compound 11 antagonizes both des-Arg⁹-BK and Lys-des-Arg⁹-BK induced contraction of the rabbit isolated aorta [13], exhibiting a notable binding affinity for the BK B1 receptor in diverse animal species. Thus, in humans its K_i is 0.034 nM [16]. Mutagenesis studies show that mutation of residues Ile-97^{2.64}, Trp-98^{ECL1}, Asn-114^{3.27}, Gln-295^{7.36}, Asp-291^{7.32} and Glu-273^{6.58} affect the binding affinity in various degrees, while mutation of Asn-298^{7.39} exhibits little impact on the binding affinity to the BK B1 receptor [15]. On the other hand, structure-activity studies suggest that the imidazole group is crucial for the high affinity of the compound, since its affinity is drastically reduced when it is substituted for a hydrophobic moiety [15]. Similarly, elimination of the fused aromatic ring of the dihydroquinoxalinone moiety reduces its affinity one order of magnitude. Finally, substitution of the sulfone by a carbonyl group reduces affinity one order of magnitude. In contrast, substitution of the dichlorophenyl moiety by a naphthyl group retains affinity.

As can be seen in Figure 4, the proposed bound conformation of compound 11 shows the dihydroimidazole group seating in a polar region surrounded by residues His-199^{5.35}, Glu-273^{6.58} and Asp-291^{7.32}. This explains the observed affinity boost produced by the addition of this moiety to the ligand [14]. The nitrogen and carbonyl groups of the dihydroquinoxalinone moiety exhibit hydrogen bonds with the sidechains of Asn-114^{3.27} and Arg-176^{4.64}, whereas the fused benzene ring exhibits as T-shaped aromatic ring-aromatic ring interaction with Tyr-266^{6.51}. Loss of the hydrogen bond interaction of the Asn-114^{3.27} explains the reduction of an order of magnitude in affinity observed in the Asn¹⁴⁴Ala mutant [15] or in the less detrimental mutation to Ser also found in the rat B1 BK receptor [15, 16]. A hydrogen bond is observed between thionyl oxygen of the sulfonamide shared between Gln-295^{7.36} and Asn-298^{7.39}. Actually, mutagenesis experiments show that mutation of Gln-295^{7.36} to alanine reduces the binding affinity of compound 11 more than one order of magnitude [15]. The other thionyl oxygen is likely involved in an intramolecular hydrogen bond with the amide group. The dichlorophenyl moiety is located in a hydrophobic pocket conformed by Trp-93^{2.60}, Ile-97^{2.64}, Trp-98^{ECL1} and Phe-101^{ECL1} and Phe-299^{7.40}. Mutagenesis analysis supports the importance of Trp-98^{ECL1} in the affinity of the compound [15]. The proposed bound conformation described above is in agreement with aforementioned SAR

and mutagenesis studies and complements further the homology model of BK B1 carried out previously using rhodopsin as template [14, 15]. Despite the two models coincide in the description of the bound conformation of compound 11, present model provides additional information about the role of diverse residues like Gln-295^{7.36} as responsible for the thionyl interaction; Asn-114^{3.27} and Arg-176^{4.64} as well as Tyr-266^{6.51} as responsible for the interaction with the dihydroquinoxalinone moiety; the involvement of Trp-93^{2.60} in the interaction with the dichlorophenyl moiety and the involvement of His-199^{5.35} in the interaction with the phenyl group, as well as the hydrogen bond between the carbonyl of the central amide group and the side chain of Arg-202^{5.38}.

Compound 12

The proposed bound conformation of compound 12 (2 in Figure 1) to the BK B1 receptor is shown in Figure 5. The molecule exhibits its 4-pyridinylpiperazinyl group interacting with several residues at the mouth of the binding pocket. Specifically, one of the nitrogens of the 4-pyridinyl moiety exhibits a hydrogen bond with the side chain of Asp-291^{7.32}, while the pyridine ring interacts with Phe-276^{6.61}. Support to the existence of an aromatic ring-aromatic ring interaction is given by the reduction of affinity observed in rats (from a K_i of 0.59 in human to 0.92 in rat), since in rat Phe-276^{6.61} is mutated to Val [17]. The smaller affinity observed can be explained to be due to the absence of the more preferred quadruple–quadruple interaction than the hydrophobic interaction. Moreover, the bridging phenyl group attached to the piperazinyl ring forms a π - π stacking with His-199^{5.35}. In the central section of the molecule the carbonyl group of the substituted urea exhibits a hydrogen bond interaction with Gln-295^{7.36} as well as the carbonyl of the diazepine ring does with Arg-202^{5.38}. Aromatic residues at the bottom left of the binding pocket (Trp-93^{2.60} and Phe-299^{7.40}) form a π - π stacking with the fused benzene ring, while the phenethyl moiety interacts with both the Trp-93^{2.60} and the Phe-101^{ECL1}.

Despite the lack of mutagenesis studies on this ligand that permit to corroborate the proposed bound conformation of compound 12, there is a limited SAR available that can be used to support present results [17]. Thus, the importance of a proton accepting center interacting with Asp-291^{7.32} is supported by the fact that elimination of the piperidine nitrogen that has attached the 4-pyridinyl group reduces drastically the affinity of the new analog, although it is recovered in part when the pyridinyl ring is replaced by a piperazine ring. It is intriguing though that substitution of the 4-pyridinyl ring by a phenyl group produces a non-binder. Our docking results predict a similar role for any of the two aromatic rings: a quadrupole-quadrupole interaction with Phe-276^{6.61} with

no specific role for the pyridinyl nitrogen, but increasing the solubility of the compound. Accordingly, we suggest as an alternative explanation that the lack of affinity observed is due to the small expected solubility of the compound.

Finally, diverse substitutions at the core benzodiazepine C-5 position show that short alkyl groups decreased affinity. In contrast, the introduction of a cyclohexyl group increased substantially affinity and furthermore, the substitution of a phenethyl group enhanced affinity by 4-fold at the human BK B1 receptor. This supports present results, since Trp-93^{2.60} and Phe-101^{ECL1} are far from the benzodiazepine ring.

NPV-SAA164

Developed by Novartis, NPV-SAA164 is an antihyperalgesic orally bioavailable B1 antagonist with K_i of 8 nM in HEK293 cells expressing human B1 receptor and no activity in rat B1 receptor [18,19]. The compound was discovered through an in-house screening of a set of non-peptide B2 antagonists that had been previously described [39]. An extensive medicinal chemistry work led to the discovery of NPV-SAA164 (3 in Figure 1) from a set of diverse analogs based on a 2-alkylamino-5-sulfamoylbenzamide core.

Figure 6 shows the proposed bound conformation of NPV-SAA164 to the BK B1 receptor. The proposed bound conformation shows the methylpiperazine group located at the mouth of the binding pocket exhibiting a hydrogen bond with the side chain of Asp-291^{7.32}. Further down, the piperidine moiety although hypothesized to act as spacer, is positioned in such a way that interacts with the aromatic imidazole ring of His-199^{5.35}. Further down along the structure, the morpholine group sits in a polar region surrounded by Arg-202^{5.38}, Tyr-266^{6.51} and Asn-298^{7.39} with a hydrogen bond interaction between the oxygen of the ring and Arg-202^{5.38} and the carbonyl group linking the morpholine and amino moiety attached to the phenylsulfonamide group interacts with Gln-295^{7.36} side chain via a hydrogen bond. The phenylsulfonamide group also interacts with both the backbone of Leu-191^{ECL2} via hydrogen bond with the sulfonyl-oxygen and the sidechain of Leu-193^{ECL2} through a van der Waals interaction. SAR studies show that the presence of an amide group increases affinity suggesting the ability to form a hydrogen bond [18]. Finally, the hydrophobic 2,2-diphenylethanamine group at the terminus of the ligand sits in the aromatic pocket of our B1 receptor model, in such a way that interacts with both the Trp-93^{2.60} at the bottom of the aromatic pocket in TM2 and Trp-98^{ECL1} and Phe-101^{ECL1}, at the top of the aromatic pocket.

Chroman 28

Chroman-28 developed by Amgen, is a potent and selective antagonist of human, non-human primate, rat, and rabbit bradykinin B1 receptors with anti-inflammatory activity and K_i between 0.7 nM at human B1 receptors [20]. Chroman 28 was developed from extensive medicinal chemistry studies devoted to optimize the spatial placement of a lipophilic sulfonamide and a basic amine moiety, previously noted to be important for high binding affinity to the B1 receptor [40].

Figure 7 shows the proposed bound conformation of Chroman 28 to the human B1 receptor. Analysis of the ligand-receptor interactions starting from the piperidine ring reveals that this moiety sits in a negatively charged region at the mouth of the receptor displaying a hydrogen bond interaction with the sidechain of Asp-297.³² SAR studies reveal that the piperidine ring can be replaced by diverse amines, being the pyrrolidine or butylamine the most active analogs. In contrast, replacement by a hydroxyl group leads to a complete loss of the affinity [41]. These results support the positioning of the piperidine ring described in the present model, since an amine can interact adequately with the diverse acid residues of the region including Asp-291^{7,32}, Glu-273^{6,58} or Glu-287^{7,28}. Replacement of an amine by a hydroxyl group generates a phenol derivative that at neutral pH will be in its basic form. This results agree well with the proposed pharmacophoric requirement for B1 antagonism mentioned above [40]. Further down the molecule, the chroman group is located close to the side chain of His-199^{5,35} interacting through a hydrogen bond between the oxygen of the chroman moiety and one of the nitrogens of the imidazole group and, also through a quadrupole-quadrupole interaction between the two rings. The model clearly justifies the differential affinity observed between the R and S enantiomers in SAR studies [41]. Further down the molecule, the amide carbonyl group exhibits a hydrogen bond with the side chain of Arg-202^{5,38} and one of the sulfonyl oxygens with the side chain of residue Gln-295^{7,36}. Interestingly, the other sulfonyl oxygen interacts with Arg-176^{4,64} located at the C-terminus of TM4 via a hydrogen bond. Moreover, the phenyl group of the aryl sulfonamide core interacts with Tyr-266^{6,51}, albeit at a bit longer distance. Improvement of this interaction led to the discovery of a sulfonamide containing a 2-oxopiperazine [42]. Finally, the naphthalene group sits in the aromatic pocket where quadruple-quadruple interactions with Trp-93^{2,60}, as well as Phe-101^{ECL1} are formed. SAR studies show that this moiety can be replaced by a trifluorobenzene without affinity loss, supporting the environment where the naphthyl group is located in the present model [42].

SSR240612

SSR240612 is a high affinity antagonist of Lys-des-Arg9 in HEK cells expressing human B1 receptor and MRC5 human lung fibroblast B1 expressing cells. Developed by Sanofi, SSR240612 was the first B1 receptor antagonist with proven efficacy and oral bioavailability in models of pain and inflammation [22, 43].

The proposed bound conformation of SSR240612 to the BK B1 receptor is shown in Figure 8. Similarly as found in Chroman 28, the nitrogen of the piperidine moiety exhibits a hydrogen bond with Asp-291^{7.32}. Further down the molecule the isopropylamide group sits in a region with several hydrophobic residues including Leu-191^{ECL2} and Leu-193^{ECL2}. In the center of the molecule, the amide group exhibits a hydrogen bond with Gln-295^{7.36}. Close to it the sulfonamide group exhibits a hydrogen bond between one of the thionyl groups and the side chain of residues Arg-176^{4.64}, whereas the other exhibits a hydrogen bond with the amide hydrogen of Leu-191^{ECL2} backbone. Attached to the sulfonamide there is a benzodioxole moiety that sits in a region with several aromatic residues including Trp-93^{2.60} and Phe-101^{ECL1}. On the other side of the molecule, the oxygen of the diaxole moiety interacts with Asn-96^{ECL1} via hydrogen bond. Finally, the methoxynaphthyl group interacts with residue Tyr-266^{6.51} and Asn-298^{7.39}.

PS020990

Discovered by PharmacoPeia from a throughput screening program using encoded combinatorial libraries, PS020990 exhibits a potent antagonist profile on human BK B1, inhibiting ³H-Des-Arg¹⁰-Kallidin at IMR-90 cells with a K₁ of 1nM [23]. PS020990 is a high selective BK B1 antagonist with a >1000-fold selectivity reported over B2R [23].

The proposed bound conformation of PS020990 is shown in Figure 9. Present docking studies reveal the imidazole ring sitting at the polar top end of the binding pocket interacting with the His-199^{5.35} and exhibits a hydrogen bond with Glu-273^{6.58}. Next to the imidazole group there is a pyridine ring that acts as spacer. It has attached a 3-chlorobenzylamine moiety that exhibits two hydrogen bond interactions, including the amine nitrogen with Arg-202^{5.38} and the chlorine of the 3-chlorobenzyl moiety with the sidechain of Asn-114^{3.27}. Further down the molecule, the carbonyl oxygen of the central amide exhibits a hydrogen bond with Gln-295^{7.36}, while the propylcyclohexane moiety sits close to Ile-190^{ECL2}. At the terminal end of the molecule the 4-chlorobenzyl group rests at the center of the aromatic site, coordinating the π-π interactions with Trp-93^{2.60} that also involves Phe-

Definition of a pharmacophore for recognition to the bradykinin B1 receptor

Comparison of the ligand-receptor complexes of the diverse antagonists used for the present study allows the definition of a pharmacophore that explains the observed structure-activity relationship observed. To define a pharmacophore of the ligand-receptor interaction, we superimposed the proposed bound structures as found in the ligand-receptor complex resulted from molecular docking studies. Analysis of the superimposed structures permitted the identification of common chemical features in similar regions of the space namely, the pharmacophoric points. For each of these pharmacophoric points an average geometric center was computed using the atomic centers of the participating atoms among the diverse antagonists. No exclusion volumes were incorporated in the pharmacophore, although the virtual screening procedure included a docking process after searching hits for pharmacophore fulfillment in order to eliminate the molecules that crashed with the receptor. The proposed pharmacophore is shown in Figure 10. It consists of five pharmacophoric points that all the ligands studied in the present study fulfil. The first point, at the polar mouth of the binding pocket, is represented by a proton donor center that complements an interaction with Asp-291^{7,32} and/or Glu-273^{6,58} and His-199^{5,35}; point 2 is either a proton donor/proton acceptor center that will interact with either Gln-295^{7,36}; point 3 is a hydrophobic ring that will interact with Trp-93^{2,60} and/or Phe-299^{7,40}; point 4 is a proton accepting center that will interact with Asn-114^{3,27} and/or Arg-176^{4,64}; point 5 is a proton donor and /or proton acceptor site that will interact with Arg-202^{5,38}, Asn-298^{7,39} and the side chain of Tyr-266^{6,51}.

All the compounds used for pharmacophore development (Figure 1) fulfil all five receptor points. It what follows we specify how specific moieties of the diverse compounds fulfil the pharmacohpric hypothesis. Thus, Compound 11 fulfils point 1 by means of the 2-phenyldihydroimidazole; point 2 by the sulfonamide oxygen; point 3 by means of the chlorophenyl moiety; point 4 by the oxygen of the dihydroquinoxalinone group and point 5 by means of by the oxygen of the amide linker group. For Compound 12, point 1 is fulfilled by the 4-pyridinepiperazine moiety; point 2 is fulfilled by means of the amide linker moiety; point 4 by both the cyclohexyl group and the benzyl moiety of the benzodiazepine and point 4 and 5 are fulfilled by the carbonyl group of the diazepine moiety. In the case of the NPV-SAA164 point 1 is fulfilled by the methyl-piperazine group nitrogen;

point 2 by means of the carbonyl group linking to the morpholine group that fulfills point 4; point 3 by both the phenyl group providing maximum coverage of the pocket side, point 5 by means of the sulfonyl oxygens of the sulfonamide. Chroman-28 covers the pharmacophore point 1 by using the chroman-7-methylpiperidine, point 2 and point 4 by means of the oxygens of the sulfonamide group; point 3 is fulfilled by the naphthalene rings and point 5 by the linker amide carbonyl group. In SSR240612 point 1 is fulfilled by the dimethyl-piperidine group; point 2 is fulfilled by the carbonyl group of the amide linker; point 3 is fulfilled by the benzodioxole moiety; while the sulphonyl oxygen fulfills point 4 and point 5 is fulfilled by the methyl-propanamide group. Finally, in the case of compound PS020990 point 1 is fulfilled by the imidazole group; point 2 by the carbonyl group of the cyclohexyl propanamide moiety; point 3 by means of the chlorophenyl group adjacent to the cyclohexyl propanamide moiety and point 5 by means of the nitrogen of the pyrimidine ring.

Proof of concept

The pharmacophore described above was later used in the discovery of novel structures with antagonistic activity for BK B1 by virtual screening. For this purpose a search was made in few databases of 3D structures of compounds including the Available Chemical Directory (ACD), the Derwent World Drug Index, the National Cancer Institute (NCI) and Maybridge for approximately 500,000 compounds. A separated searches for compounds fulfilling five, four and three pharmacophoric points yielding a large set of compounds was carried out. A selected group of them were purchased and tested for their BK B1 antagonistic activity.

Biological assays permitted to identify new highly diverse hits with structures that do not resemble those used for pharmacophore development. The success rate achieved to identify new hits with an antagonistic activity by virtual screening was approximately one third of the selected molecules, as previously found by other authors [44]. Table 1 shows the structures as well as the antagonistic activity to the human bradykinin BK B1 of a selected group of hits that are disclosed to give support to the pharmacophoric hypothesis developed in this work. These molecules were docked onto the receptor model and inspected for fulfilment of the pharmacophore. Information regarding the number of pharmacophoric points fulfilled by each of the hits is also included in Table 1. Interestingly, the antagonistic activity observed experimentally correlates well with the number of pharmacophoric points fulfilled by these molecules.

As an example, Figure 11 shows compound #10 bound to the BK B1 showing the fulfilment of the

pharmacophoric points. The ligand is shown to fulfil 3 pharmacophoric points 1, 3 and 5. The charged amine moiety interacts with the Asp-291^{7,32}, and thus fulfilling point 1, the indole group nest deep in the hydrophobic pocket and fulfils point 3 and finally the nitrile group fulfils point 5 by interacting via hydrogen bond with both the sidechain of Tyr-266^{6,51} and Arg-202^{5,38}. While the molecule have other polar groups such as carbonyl that could interact with Gln-295^{7,36} and Asn-114^{3,27}, the size and conformation of these moieties and the compound in general, are not adequate enough to orient in a suitable manner for proper interactions. This emphasizes the reason why most of the BK B1 antagonists published are big as they need to span out to all pharmacophoric points to suitably interact.

Conclusions

Models of the bound conformation of diverse non-peptide human BK B1 antagonists were constructed and the stereochemical features of the complexes were analyzed with the aim to find common trends. To accomplish this, an atomistic model of the receptor was constructed by homology modeling, using the human CXC4 chemokine and bovine rhodopsin receptor as template (chimeric template). Antagonists selected for the present study included Compound 11, Compound 12, NPV-SAA164, Chroman-28, SSR240612 and PS020990, covering the maximum possible diversity. Complexes with the bound conformation of each of the antagonists were constructed by docking the molecules into the receptor. Due to the flexibility of the ligands and the size of the orthosteric site of the receptor, several docking attempts were carried out for each of the molecules. The final conformation was selected by the scoring function and the results of both SAR and site directed mutagenesis studies available in the published literature.

Our results suggest that there are certain anchoring points that are found in more than one compound permitting the definition of a common pharmacophore. This consist of five points that defined on the features of the ligand include proton donor (point 1); a proton acceptor/proton donor center (point 2); a hydrophobic ring (point 3); proton acceptor/proton donor center (point 4) and proton donor/proton acceptor.

The pharmacophore was used in a subsequent study to guide a virtual screening process. The results permitted to identify a set of compounds some of which were purchased and *in vitro* tested for their capability to antagonize the BK B1. Consequently, a subset of compounds with highly diverse structures that give support to the validity of the pharmacophoric hypothesis described in this work was also disclosed.

References

1. Hall JM (1992). Bradykinin receptors: pharmacological properties and biological roles *Pharmacol Therapeutics* 56: 131-190.
2. Regoli D, Barabe J (1980) Pharmacology of bradykinin and related kinins *Pharmacol Rev* 32: 1-46.
3. Leeb-Lundberg L M F, Marceau F, Muller-Esterl W, Pettibone D J, Zuraw B L (2005) International Union of Pharmacology. XLV. Classification of the Kinin Receptor Family: from Molecular Mechanisms to Pathophysiological Consequences *Pharmacol Rev* 57: 27-77.
4. Stewart J (1995) Bradykinin Antagonists: Development and Applications *Biopolymers (Peptide Science)* 37: 143-155.
5. Hock F J, Wirth K, Albus U, Linz W, Gerhards G H, Wiemer G, Henke S, Breipohl G, Konig W, Knolle J, Scholkens B A (1991) Hoe 140 a New Potent and Long-Acting Bradykinin-Antagonist: in vitro Studies *Br J Pharmacol* 102: 769-773.
6. Cole S W, Lundquist L M. (2013) Icatibant for the treatment of hereditary angioedema. *Ann Pharmacother* 47: 49-55.
7. Marceau F (1995) Kinin B1 Receptors: A Review *Immunopharmacol* 30: 1-26.
8. Ahluwalia A, Perretti M (1999) B 1 receptors as a new inflammatory target. Could this B the 1? *Trends Pharmacol Sci* 20: 100-104.
9. Dray A (1995) Inflammatory mediators of pain *Br J Anaesth* 75: 125-131.
10. Biswas K, Aya T, Qian W, Peterkin T A, Chen J J, Human J, Hungate RW, Kumar G, Arik L, Lester-Zeiner D, Biddlecome G, Manning BH, Sun H, Dong H, Huang M, Loeloff R, Johnson EJ, Askew BC (2008) Aryl sulfones as novel bradykinin B1 receptor antagonists for treatment of chronic pain *Bioorg Med Chem Lett* 18: 4764-4769.
11. Wong C T, Rowlands D K, Wong C H, Lo T W, Nguyen G K, Li H Y, Tam J P (2012) Orally active peptidic bradykinin B1 receptor antagonists engineered from a cyclotide scaffold for inflammatory pain treatment *Angew Chem* 124: 5718-5722.
12. Chen J J, Johnson E J (2007) Targeting the bradykinin B1 receptor to reduce pain *Expert Opin Ther Targets* 11:21-35.
13. Campos M M, Leal P C, Yunes R A, Calixto J B (2006) Non-peptide antagonists for kinin B 1 receptors: new insights into their therapeutic potential for the management of inflammation and pain *Trends Pharmacol Sci* 27: 646-651.
14. Su D S, Markowitz M K, DiPardo R M, Murphy K L, Harrell C M, O'Malley S S, Ransom R W, Chang R S, Ha S, Hess F J, Pettibone D J, Mason G S, Boyce S, Freidinger RM, Bock M G (2003) Discovery of a potent, non-peptide bradykinin B1 receptor antagonist *J Am Chem Soc* 125: 7516-7517.
15. Ha S N, Hey P J, Ransom R W, Harrell C M, Murphy K L, Chang R, Chen T B, Su D S, Markowitz M K, Bock M G, Freidinger R M, Hess F J (2005) Binding modes of dihydroquinoxalinones in a homology model of bradykinin receptor 1 *Biochem Biophys Res Comm* 331: 159-166.

16. Morissette G, Fortin J P, Otis S, Bouthillier J, Marceau F (2004) A novel nonpeptide antagonist of the kinin B1 receptor: effects at the rabbit receptor *J Pharmacol Exp Ther* 311: 1121-1130.
17. Wood M R, Kim J J, Han W, Dorsey B D, Hornick C F, DiPardo R M, Kuduk S D, MacNeil T, Murphy K L, Lis E V, Ransom R W, Stump G L, Lynch J J, O'Malley S S, Miller P J, Chen T B, Harrell C M, Chang R S, Sandhu P, Ellis J D, Bondiskey P J, Pettibone D J, Freidinger R M, Bock M G (2003) Benzodiazepines as potent and selective bradykinin B1 antagonists *J Med Chem* 46: 1803-1806.
18. Ritchie T J, Dziadulewicz E K, Culshaw A J, Müller W, Burgess G M, Bloomfield G C, Drake G S, Dunstan A R, Beattie D, Hughes G A, Ganju P, McIntyre P, Bevan S J, Davis C, Yaqoob M (2004) Potent and orally bioavailable non-peptide antagonists at the human bradykinin B1 receptor based on a 2-alkylamino-5-sulfamoylbenzamide core *J Med Chem* 47: 4642-4644.
19. Fox A, Kaur S, Li B, Panesar M, Saha U, Davis C, Dragoni I, Colley S, Ritchie T, Bevan S, Burgess G, McIntyre P (2005) Antihyperalgesic activity of a novel nonpeptide bradykinin B1 receptor antagonist in transgenic mice expressing the human B1 receptor *Br J Pharmacol* 144: 889-899.
20. D'Amico D C, Aya T, Human J, Fotsch C, Chen J J, Biswas K, Riahi B, Norman M H, Willoughby C A, Hungate R, Reider P J, Biddlecome G, Lester-Zeiner D, Staden C V, Johnson E, Kamassah A, Arik L, Wang J, Viswanadhan V N, Groneberg R D, Zhan J, Suzuki H, Toro A, Mareska D A, Clarke D E, Harvey D M, Burgess L E, Laird E R, Askew B, Ng G (2007) Identification of a nonpeptidic and conformationally restricted bradykinin B1 receptor antagonist with anti-inflammatory activity *J Med Chem* 50: 607-610.
21. Chen J J, Qian W, Biswas K, Viswanadhan V N, Askew B C, Hitchcock S, Hungate R W, Arik L, Johnson E (2008) Discovery of dihydroquinoxalinone acetamides containing bicyclic amines as potent Bradykinin B1 receptor antagonists *Bioorg Med Chem Lett* 18: 4477-4481.
22. Gougat J, Ferrari B, Sarran L, Planchenault C, Poncelet M, Maruani J, Alonso R, Cudennec A, Croci T, Guagnini F, Urban-Szabo K, Martinolle J P, Soubrié P, Finance O, Le Fur G (2004) SSR240612 [(2R)-2-[(3R)-3-(1,3-benzodioxol-5-yl)-3-[[6-methoxy-2-naphthyl]sulfonyl]amino]propanoyl]amino]-3-(4-[[2R,6S)-2,6-dimethylpiperidinyl]methyl]phenyl)-N-isopropyl-N-methylpropanamide hydrochloride], a new nonpeptide antagonist of the bradykinin B1 receptor: biochemical and pharmacological characterization *J Pharmacol Exp Ther* 309:661-669.
23. Horlick R A, Ohlmeyer M H, Stroke I L, Strohl B, Pan G, Schilling A E, Paradkar V, Quintero J G, You M, Riviello C, Thorn M B, Damaj B, Fitzpatrick V D, Dolle R E, Webb M L, Baldwin J J, Sigal N H (1999) Small molecule antagonists of the bradykinin B1 receptor *Immunopharmacol* 43: 169-177.
24. Wu B, Chien E Y, Mol C D, Fenalti G, Liu W, Katritch V, Abagyan R, Brooun A, Wells P, Bi F C, Hamel D J, Kuhn P, Handel T M, Cherezov V, Stevens R C (2010) Structures of the CXCR4 chemokine GPCR with small-molecule and cyclic peptide antagonists *Science* 330: 1066-1071.
25. Rosenbaum D M, Rasmussen S G, Kobilka B K (2009) The structure and function of G-protein-coupled receptors *Nature* 459: 356-363.

26. Li J, Edwards P C, Burghammer M, Villa C, Schertler G F (2004) Structure of bovine rhodopsin in a trigonal crystal form *J Mol Biol* 343: 1409-1438.
27. Sali A, Blundell T L (1993) Comparative protein modelling by satisfaction of spatial restraints *J Mol Biol* 234: 779–815.
28. Molecular Operating Environment (MOE). Chemical Computing Group Inc. 1010 Sherbooke St. West Suite #910 Montreal QC Canada H3A 2R7.
29. Friesner R A, Banks J L, Murphy R B, Halgren T A, Klicic J J, Mainz D T, Repasky M P, Knoll E H, Shaw D E, Shelley M, Perry J K, Francis P, Shenkin P S (2004) Glide: A New Approach for Rapid Accurate Docking and Scoring. 1. Method and Assessment of Docking Accuracy *J Med Chem* 47: 1739–1749.
30. Cordomi A, Edholm O, Perez J J (2007) Effect of different treatments of long-range interactions and sampling conditions in molecular dynamic simulations of rhodopsin embedded in a dipalmitoyl phosphatidylcholine bilayer *J Comput Chem* 28: 1017-1030.
31. Van Der Spoel D, Lindahl E, Hess B, Groenhof G, Mark A E, Berendsen H J (2005) GROMACS: fast flexible and free *J Comp Chem* 26: 1701–1718.
32. Friesner R A, Murphy, R B, Repasky M P, Frye L L, Greenwood J R, Halgren T A, Sanschagrin P C, Mainz DT (2006) Extra Precision Glide: Docking and Scoring Incorporating a Model of Hydrophobic Enclosure for Protein-Ligand Complexes *J Med Chem* 49: 6177–6196.
33. Jones C, Phillips E, Davis C, Arbuckle J, Yaqoob M, Burgess G M, Docherty R J, Webb M, Bevan S J, McIntyre P (1999) Molecular characterisation of cloned bradykinin B 1 receptors from rat and human. *Eur J Pharmacol* 374: 423-433.
34. Lupala C S, Rasaeifar B, Gomez-Gutierrez P, Perez J J (2015). Effect of template selection on the construction of atomistic models of GPCRs by homology modeling *J Biomol Struct Dyn* 33 (Sup1): 127-128.
35. Mobarec J C, Sanchez R, Filizola M (2009) Modern homology modeling of G-protein coupled receptors: which structural template to use? *J Med Chem* 52: 5207-5216.
36. Krieger E, Joo K, Lee J, Lee J, Raman S, Thompson J, Tyka M, Baker D, Karplus K (2009) Improving physical realism, stereochemistry, and side-chain accuracy in homology modeling: four approaches that performed well in CASP8 *Proteins* 77: 114-122.
37. Katritch V, Cherezov V, Stevens R C (2012) Diversity and modularity of G protein-coupled receptor structures *Trends Pharmacol Sci* 33: 17-27.
38. Ballesteros
39. Dziadulewicz E K, Ritchie T J, Hallett A, Snell C R, Davies J W, Wigglesworth R, Dunstan A R, Bloomfield G C, Drake G S, McIntyre P, Brown M C, Burgess G. M, Lee W, Davis C, Yaqoob M, Phagoo S B, Phillips E, Perkins M N, Campbell E A, Davis A J, Rang H P (2002) Nonpeptide Bradykinin B2 Receptor Antagonists: Conversion of Rodent-Selective Bradyzide Analogues into Potent Orally-Active Human Bradykinin B2 Receptor Antagonists *J Med Chem* 45: 2160-2172.

40. Marceau F (2005) A possible common pharmacophore in the non-peptide antagonists of the bradykinin B1 receptor *Trends Pharmacol Sci* 26:116-118.
41. Biswas K, Li A, Chen J J, D'Amico D C, Fotsch C, Han N, Human J, Liu Q, Norman M H, Riahi B, Yuan C, Suzuki H, Mareska D A, Zhan J, Clarke D E, Toro A, Groneberg R D, Burgess L E, Lester-Zeiner D, Biddlecome G, Manning B H, Arik L, Dong H, Huang M, Kamassah A, Loeloff R, Sun H, Hsieh F Y, Kumar G, Ng G Y, Hungate R W, Askew B C, Johnson E (2007) Potent nonpeptide antagonists of the bradykinin B1 receptor: structure-activity relationship studies with novel diaminochroman carboxamides *J Med Chem* 50: 2200-2212.
42. Biswas K, Peterkin T A N, Bryan M C, Arik L, Lehto S G, Sun H, Hsieh F-Y, Xu C, Fremeau R T, Allen J R (2011) Discovery of Potent, Orally Bioavailable Phthalazinone Bradykinin B1 Receptor Antagonists *J Med Chem* 54: 7232–7246.
43. Pietrovski E F, Otuki M F, Regoli D, Bader M, Pesquero J B, Cabrini D A, Zampronio A R (2009) The non-peptide kinin receptor antagonists FR 173657 and SSR 240612: preclinical evidence for the treatment of skin inflammation *Regul Peptides* 152: 67-72.
44. Krishna S, Singh D K, Meena S, Datta D, Siddiqi M I, Banerjee D (2014) Pharmacophore-Based Screening and Identification of Novel Human Ligase I Inhibitors with Potential Anticancer Activity *J Chem Inf Model* 54: 781–792.

Captions to the Figures

Figure 1: Chemical structures of the B1 antagonists studied in the present work. Compound 11 (1), Compound 12 (2), NPV-SAA164 (3), Chroman28 (4), SSR240612 (5) and PS020990 (6).

Figure 2: Sequence alignment of human B1 receptor (bottom) with human CXC4 chemokine receptor and bovine receptors (for part in TM7 and TM8). Transmembrane segments are inserted in boxes colored in green.

Figure 3: (a) Lateral view of the orthosteric binding pocket of the human B1 bradykinin receptor modeled in complex with compound 11, (b) same as (a) viewed from the extracellular side (aerial).

Figure 4. Pictorial view of the proposed binding mode of Compound 11 bound to the BK B1 receptor.

Figure 5: Pictorial view of the proposed binding mode of Compound 12 bound to the BK B1 receptor.

Figure 6: Pictorial view of the proposed binding mode of NPV-SAA164 bound to the BK B1 receptor.

Figure 7: Pictorial view of the proposed binding mode of Chroman 28 bound to the BK B1 receptor.

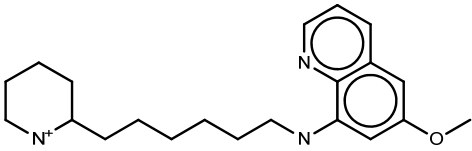
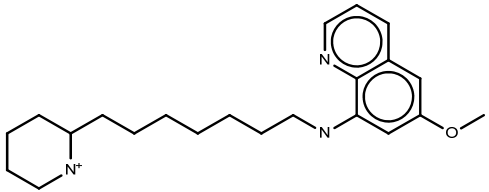
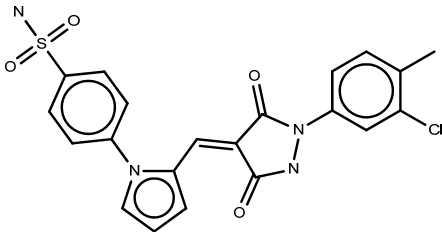
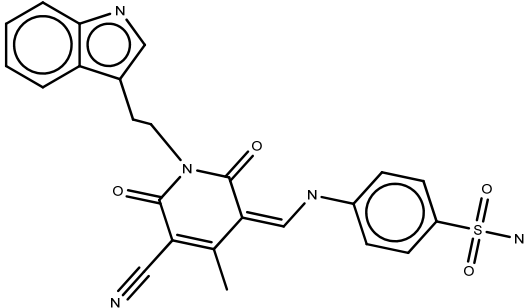
Figure 8: Pictorial view of the proposed binding mode of SSR240612 bound to the BK B1 receptor.

Figure 9: Pictorial view of the proposed binding mode of PS020990 bound to the BK B1 receptor.

Figure 10: Proposed pharmacophore for the BK B1 antagonism. Distance between pharmacophoric points are: $d(1,2)= 9.2 \text{ \AA}$; $d(1,3)=13.1$; $d(1,4)= 1.5$; $d(1,5)=9.5$; $d(2,3)=5.1$; $d(2,4)=7.6.$; $d(2,5)=9.3$; $d(3,4)=7.8$; $d(3,5)=9.5$; $d(4,5)=5.7$

Figure 11: Pictorial view of compound #9 of Table 4.2 bound to the BK B1 receptor with the pharmacophore points represented as spheres of different colors.

Table 1. Structures of the new hits discovered together with their antagonistic effect towards the human BK B1 receptor and the number of pharmacophore points fulfilled.

Structure	Inhibition	Pharmacophore points
 <p>Compound #7</p>	31% @ 50 μ M	2 (points 1 and 3)
 <p>Compound #8</p>	46% @ 50 μ M	2 (points 1 and 3)
 <p>Compound #9</p>	31% @ 10 μ M	3 (points 1, 2 and 3)
 <p>Compound #10</p>	32% @ 10 μ M	3 (points 1, 3 and 5)